Anomaly Detection in Molecular Communications With Applications to Health Monitoring Networks

Siavash Ghavami, *Member, IEEE*

***Abstract*—Early detection of diseases such as cancer plays a crucial role in their successful treatment. Motivated by this, anomaly detection in molecular nano-networks is studied. The proposed anomaly detection is, in fact, a two-tier network of artificial cells (ACs) in the first tier and a bio-cyber interface (BC) in the second tier. The ACs detect anomaly by variation in concentration of the biomarker molecules released by diseased cells (DCs) to the channel ending to ACs. This channel is modeled by a molecular communication (MC) paradigm. In the second tier, the ACs transmit a molecular message to a BC through the cardiovascular network, which is modeled again by the MC paradigm. A decision is made in the BC, which is implemented on the body skin, based on the received messages from different ACs. Due to the nature of the problem, a suboptimum design of detectors in the first and second tiers are provided. We use a Neyman-Pearson (NP) framework to analyze the detection performance of a health monitoring network. Based on bounding likelihood ratio (LR) a lower bound for the probability of detection and an upper bound for false alarm of each AC is derived. Next, taking into account the effect of ACs-BC channels, the overall performance of anomaly detection is analyzed in terms of probabilities of detection and false alarm.**

***Index Terms*—Health monitoring network, anomaly detection, artificial cell, molecular communication, in vivo networking.**

I. Introduction

DETECTION of nano-scale anomalies in a bio-molecular environment is a vital task of health monitoring networks [1]. Anomaly detection in practical bio-molecular settings, typically comprises a two-tier network architecture. In the first tier, the presence of anomaly is detected at the nano-scale level using nanosensors. In the second tier, the anomaly is reported at a larger scale to the outside world [2].

The networked system for anomaly detection contains nano-size communicating gadgets, capable of working inside the human body. For instance they might be responsible for measuring the level of glucose in the blood, monitoring the digestive tract through pill-sized ingestible cameras or monitoring bone growth for diabetes treatment [3]. The sensing range of each nanosensor is restricted to its close nano-environment, thus numerous nanosensors are expected to cover noteworthy areas or volumes. Moreover, existence an external device and the sensor cooperation are important to pursue the status of the patient [4]. By means of communications, nanosensors will be able to autonomously transmit their sensing information in a multi or single-hop fashion to a common sink, react to instructions from a command center, or coordinate joint actions when required [1]. The resulting anomaly detection network will enable smart health monitoring and drug delivery system design.

First, we review the current literature on anomaly detection in molecular communication. Next review networked decision making for inhomogeneous Poisson point process. Modeling anomaly detection in MC using the Poisson point process is an objective of this paper to capture the time-varying nature of Anomaly detection based on MC. Two-tier anomaly detection in bio-molecular environment is investigated in [2], [4]–[9]. In [5], [6] a two-tier network for breast cancer detection is proposed. In the first tier, the injected molecules interact with cancer cells and in the second tier the resulting chemical of this interaction is detected by imaging techniques. In the early detection of lung cancer, the increased level of epidermal growth factor receptor (EGFR) can react at the nanoscale with injected single chain forward variable (SCFV) polypeptide with embedded Au [7]. Next, the product of this reaction may be recognized by imaging techniques for finding Au in the body [8]. In [2] and [9] a two-tier nano anomaly detection scheme, where the nanosensors have homogenous Poisson and Gaussian observations, respectively, are suggested and their detection performance are analyzed. In [10] early cancer detection in blood vessels using mobile nanosensors has been addressed. Abnormality detection inside blood vessels with mobile nanomachines is investigated in [11]. Advanced target detection via molecular communication has been discussed in [12]. A distributed cooperative detection scheme for multi-receiver molecular communication has recently been presented in [13]. A cooperative abnormality detection via diffusive molecular communications has been considered in [14]. A symbol-by-symbol maximum likelihood detection for cooperative molecular communication has been proposed in [15]. Recently, in [16], authors investigated the problem of detecting and monitoring changes (abnormality) in molecular communication (MC), using the quickest change detection schemes to minimize the delay of detection. In [17], molecules propagation according to anomalous diffusion instead of the conventional Brownian motion has been identified using reinforcement learning. Cardiovascular system monitoring via wireless nano sensor networks has

Manuscript received November 6, 2019; revised March 15, 2020; accepted June 11, 2020. Date of publication June 19, 2020; date of current version July 15, 2020. The associate editor coordinating the review of this article and approving it for publication was W. Guo.

The author is with the Department of Electrical and Computer Engineering, University of Minnesota, Minneapolis, MN 55455 USA (e-mail: siavash.ghavami@gmail.com).

This article has supplementary downloadable material available at http://ieeexplore.ieee.org, provided by the author.

Digital Object Identifier 10.1109/TMBMC.2020.3003877

been studied in [18]. Moreover, silent entity localization using machine learning based method has been studied in [19], which can be considered as a next procedure after anomaly detection.

Networked decision making for inhomogeneous Poisson point processes with applications to nuclear detection is proposed in [20]–[26] to detect the presence of an inhomogeneous Poisson process superimposed with Poisson noise. Decision making accuracy for sensor networks with inhomogeneous Poisson observations is considered in [26]. Upper bound of false alarm probability and lower bound of detection probability of nuclear detection problem is considered in [20], [25], [26]. Error probability bounds for nuclear detection is also considered in [22]–[24].

The communication link in the first tier of anomaly detection network naturally should be modeled by the diffusion-based MC paradigm [27]. However, for the second tier, one may consider the recent proposals of wireless nanosensor networks including: diffusion-based MC [27], ultrasonic communications [3], [28] or optical [29] communication techniques. One of the propositions, which recommends the molecular communication for AC-BC communication, expect the cardiocirculatory framework to be the transmission medium [30]. This proposition utilizes a number of mobile, circulating nanomachines, which act as sensors, and a smart, fixed probe, arranged along a blood vessel, which go about as the sink for the data gathered by the sensors. After the probe has received explicit signals from the circulating nanomachines, it conveys their data information to the Bio-Cyber interface.

In this paper, both tiers are modeled based on diffusion-based MC paradigm over a cardiovascular network. Anomaly detection setting includes a set of artificial cells (ACs) randomly deployed inside the body. These ACs are responsible for measuring biomarker[1] concentration over a MC channel between the diseased cells (DCs) and ACs. If the biomarker concentration deviates from the normal value, the ACs alarm the presence of anomaly. The ACs communicate their decisions by releasing molecules over another MC channel towards a bio-cyber interface (BC). Fusing the collected molecular signals, the BC makes a decision and may alarm the presence of an anomaly as necessary.

This paper consider an inhomogeneous Poisson point process to model the number of received biomarker molecules at each AC. In comparison with the literature of detection of inhomogeneous Poisson point process such as nuclear detection [20]–[26], the contributions of this work are as follows: The complex nature of molecular environment imposes a more complex hypothesis test, which cannot be modeled only with presence of an inhomogeneous Poisson point process such as [20]. The detection performance of hypothesis testing of such complex hypothesis test has been addressed here. The effect of noise is considered in both DC-AC and AC-BC links.

In this paper, a lower bound of detection probability and an upper bound of false alarm of the ACs are derived by bounding the likelihood ratio (LR), where will be used in the Neyman-Pearson (NP) framework. Next, incorporating the effect of ACs-BC channels, the total detection performance of health monitoring network is analyzed. Then, the presented analysis uses a NP framework to obtain the optimized thresholds in the ACs and BC to maximize the lower bound of the probability of detection in a given false alarm probability. Extensive numerical tests are provided to quantify the effect of different design and system parameters on the anomaly detection performance of the proposed health monitoring network.

The outline of this paper is as follows. In Section II, the system model of health monitoring network and problem statement are presented. The performance of Hypothesis test for anomaly detection at ACs is described in Section III. The performance of anomaly detection at BC is analyzed in Section IV. Section V provides numerical tests and finally Section VI concludes this paper.

II. System Model and Problem Statement

Health monitoring network includes a two-tier structure for anomaly detection in the first tier and reporting the anomaly in the second tier. The structure of two-tier anomaly detection network has been shown in Fig. 1(a), block diagram of the network is depicted in Fig. 1(b). In our system model, the MC paradigm models the in vivo communications over both the first and second tiers [27]. In the first tier the DCs and ACs are considered as transmitters and receivers, respectively. It is assumed that the DCs are concentrated in a specific unknown location inside the body, releasing biomarker molecules. The released biomarker molecules propagating throughout the body via blood vessels are expected to be absorbed by the ACs near to DCs. If the concentration of the received biomarker molecules in a specific AC deviates from the normal level, the AC alarms the presence of anomaly by releasing molecules into the cardiovascular network. In the second tier the BC is alarmed by the released molecules of the ACs. Fusing the collected molecular signals, the BC makes a decision and may alarm the presence of an anomaly as necessary. The more detailed description of the proposed model is provided in the following Subsections.

A. DCs-AC System Model

The DCs release biomarker molecules into the blood vessels. This release procedure might be due to the shedding of endothelial cells from the arterial wall in the case of a heart attack [31]. The release process of biomarkers is frequently modeled by the Weibull function [32]. It models the transmit waveform of biomarkers over time as

$$x_D(t) = x_{D_0}\Big(1 - \exp\Big(-\kappa t^b\Big)\Big). \tag{1}$$

where x_{D_0} is the released biomarker concentration at infinity ($t \to +\infty$), b is the unitless biomarker power-law coefficient, which depends on the mass transport of the medium, and $\kappa > 0$ is the biomarker release coefficient.

The released biomarkers go throughout the body via the blood vessels. For the sake of tractability consider a time slotted based system. Then, the received number of biomarkers in

[1]Biomarkers are molecules in an organism whose presence is indicative of some phenomenon such as a disease or infection.

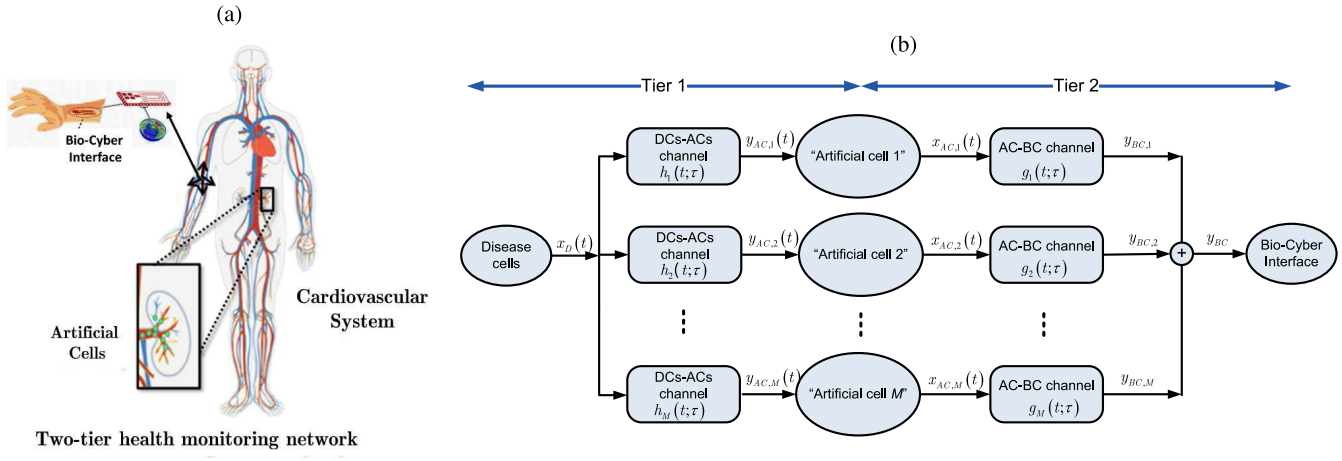

Fig. 1. (a) Anomaly detection inside the body (b) Illustration of the proposed two-tier health monitoring network.

the n^{th} time slot at the m^{th} AC can be modeled by [33]

$$y_{AC,m}[n] = \text{Poiss}\big(p_r \lambda_{AC,m}[n] + p_r \bar{\eta}_m\big) \tag{2}$$

where p_r is the probability of reception, $\bar{\eta}_m$ is the mean of Poisson noise, and $\lambda_{AC,m}[n]$ is average number of biomarker molecules receive at the m^{th} AC. The $\lambda_{AC,m}[n]$ is given by [33]

$$\lambda_{AC,m}[n] = \int_{(n-1)T_s}^{nT_s} \int_{t-L^{(h_m)}T_s}^{t} h_m(t;\tau) x_D(\tau) d\tau dt \tag{3}$$

where $h_m(t;\tau) > 0$ is the time varying channel between DCs, and the m^{th} AC at transmission time τ, and reception time t. Therefore, the propagation probability of receiving molecules on n^{th} time slot from transmitted molecules in $n-l$ previous time slot, is given by

$$h_m[n,l] = \int_{(n-1)T_s}^{nT_s} dt \int_{-\infty}^{t} p_r(t) h(t,\tau) \delta(\tau - lT_s) \tag{4}$$

The memory length of the channel between the DCs and the m^{th} AC, is denoted by $L^{(h_m)}$ and T_s is sampling period. The $h_m[n,l]$ is equal to [35]

$$h_m[n,l] = \begin{cases} F_{W,m}(nT_s, lT_s) - F_{W,m}(nT_s, (l-1)T_s) & l \le L^{h_m} \\ 0 & l \ge L^{h_m} \end{cases} \tag{5}$$

where $F_{W,m}(t,w)$ is the cumulative distribution function (CDF) of the propagation time which is obtained using an additive inverse Gaussian (AIG) analysis in [34]. Since, each molecule defuses as a Brownian motion process until it reaches a certain distance, at which point it is detected. Propagation of molecules depends on the drift velocity, $v_m(t)$, the Brownian motion variance $\sigma_m^2(t)$ and the distance between DC and m^{th} AC, l_m. Hence, $F_{W,m}(t,w)$ is given by [34]

$$F_{W,m}(t,w) = \Phi\left(\sqrt{\frac{\lambda_m(t)}{w}}\left(\frac{w}{\mu_m(t)} - 1\right)\right) + e^{\frac{2\lambda_m(t)}{\mu_m(t)}} \Phi\left(-\sqrt{\frac{\lambda_m(t)}{w}}\left(\frac{w}{\mu_m(t)} + 1\right)\right) \tag{6}$$

in which, $\mu_m(t) = l_m / v_m(t)$, $\lambda_m(t) = (l_m^2)/\sigma_m^2(t)$, $\sigma_m^2(t) = (\delta_m(t))/2$ is the variance of the associated Weiner process, $\delta_m(t)$ is the coefficient of diffusion between m^{th} AC and BC at time t [34], and $\Phi(.)$ is the CDF of a standard Gaussian random variable. We assume that, $v_m(t)$ and $\delta_m(t)$ are constant over at least $L^{(h_m)}T_s$ second to (6) is valid. Each molecule defuses as a Brownian motion process until it reaches a certain distance, at which point it is detected. Therefore, the probability of receiving a molecule in same time slot is $F_W(t, T_s)$.

B. ACs-BC System Model

The second tier aims to report the anomaly to the BC through a MC channel. In this tier, if the m^{th} AC detects anomaly, it will report to the BC by releasing $x_{AC,m}(t)$ molecules into the cardiovascular network. The release process of molecules by ACs can be motivated by the Weibull function [32], which is given by

$$x_{AC,m}(t) = x_{AC_0} \exp\left(-\kappa' t^{b'}\right) \tag{7}$$

where x_{AC_0} is the transmitted molecules concentration at $t = 0$, k' and b' are biomarker release and unitless biomarker power law coefficients of ACs, respectively. If AC does not detect anomaly it will not release anything. The number of received molecules at the BC through the molecular ACs-BC channel is

$$y_{BC} = \sum_{m=1}^{M} \text{Poiss}\big(q_r \lambda_{BC,m}\big) + \text{Poiss}(q_r \bar{\varepsilon}) \tag{8}$$

where q_r, $\bar{\varepsilon}$ and M are reception probability and mean of Poisson noise at the BC and the number of ACs, respectively. $\lambda_{BC,m}$ is the average number of received molecules from the m^{th} AC, and it is given by

$$\lambda_{BC,m} = \int_{0}^{T_{BC}} \int_{t-L^{(g_m)}T_s}^{t} g_m(t;\tau) x_{AC,m}(\tau) d\tau dt \tag{9}$$

where $g_m(t;\tau) > 0$ is the channel between m^{th} AC and the BC, and $L^{(g_m)}$ is the memory length of the m^{th} channel in the second tier, and T_{BC} is the time duration of decision at BC.

TABLE I
DESCRIPTION OF SYSTEM PARAMETERS

Parameter	Description
$x_D(t)$	Released molecules by DCs at time t
$h_m(t;\tau)$	The MC channel between the DCs and m^{th} AC at reception time t and transmission time τ
$y_{AC,m}(t)$	No. of received molecules by the m^{th} AC
$\lambda_{AC,m}[n]$	Ave. no. of received molecules at m^{th} AC during n^{th} time slot
$x_{AC,m}(t)$	Released molecules by the m^{th} AC
$g_m(t;\tau)$	The MC channel between the m^{th} AC and BC at reception time t and transmission time τ
$y_{BC,m}(t)$	No. of received molecules by the BC from the m^{th} AC
$\lambda_{BC,m}$	Ave. no. of received molecules from the m^{th} AC
y_{BC}	Received molecules by the BC

C. Hypothesis Test for Anomaly Detection

In this subsection the hypothesis test based on which the ACs identify anomaly is proposed as follows

$$\begin{cases} \mathcal{H}_0: \ x^{\mathcal{H}_0,\min} \le x_{D_0} \le x^{\mathcal{H}_0,\max} \\ \mathcal{H}_1: \ \begin{cases} \mathcal{H}_1^-: \ x_{D_0} \le x^{\mathcal{H}_1^-,\max} \\ \mathcal{H}_1^+: \ x_{D_0} \ge x^{\mathcal{H}_1^+,\min} \end{cases} \end{cases} \tag{10}$$

where $x^{\mathcal{H}_0,\max}$ and $x^{\mathcal{H}_0,\min}$ denote the maximum and minimum values of biomarker concentration in the healthy setting ($\mathcal{H}_0$). $x^{\mathcal{H}_1^-,\max}$ and $x^{\mathcal{H}_1^+,\min}$ correspond to the maximum and minimum values of biomarker concentration in the non-healthy setting $\mathcal{H}_1^+$ and $\mathcal{H}_1^-$ respectively. $\mathcal{H}_1^-$ and $\mathcal{H}_1^+$ are subsets of $\mathcal{H}_1$ and an illustration of them are depicted in Fig. 2.

Decision on the presence of anomaly has been taken when $x_D(t)$ approaches steady-state; that is $t - L^{(h_m)}T_s > t_{ss}$. t_{ss} is the minimum time, t, satisfying

$$\left|x_D(t_{ss}) - x_{D_0}\right| \le \zeta \tag{11}$$

where ζ is an arbitrarily small positive quantity. In addition, let us define $n_{ss} \coloneqq \lfloor t_{ss}/T_s \rfloor$ as the minimum sampling index for the steady state.

Further, let $\lambda_{AC,m}[n]$ as the average number of received biomarkers at the m^{th} AC during n^{th} time-slot. Due to the time varying nature and positivity of $h_m(t;\tau)$, and for the sake of tractability, consider $\lambda_{AC,m}^{\mathcal{H}_0,\min}$ and $\lambda_{AC,m}^{\mathcal{H}_0,\max}$ as a lower and upper bounds for the $\lambda_{AC,m}[\,\cdot\,]$ under hypothesis test of $\mathcal{H}_0$. Similarly, consider $\lambda_{AC,m}^{\mathcal{H}_1^+,\min}$ and $\lambda_{AC,m}^{\mathcal{H}_1^-,\max}$ as a lower and upper bounds for the $\lambda_{AC,m}[\,\cdot\,]$ under hypothesis test of $\mathcal{H}_1^+$ and $\mathcal{H}_1^-$ respectively, i.e., $\forall n \in \{n_{ss}+1,\ldots,n_{ss}+N\}$ we have

$$\begin{cases} \mathcal{H}_0: \ \lambda_{AC,m}^{\mathcal{H}_0,\min} \le \lambda_{AC,m}[n] \le \lambda_{AC,m}^{\mathcal{H}_0,\max} \\ \mathcal{H}_1: \ \begin{cases} \mathcal{H}_1^-: \ \lambda_{AC,m}[n] \le \lambda_{AC,m}^{\mathcal{H}_1^-,\max} \\ \mathcal{H}_1^+: \ \lambda_{AC,m}[n] \ge \lambda_{AC,m}^{\mathcal{H}_1^+,\min} \end{cases} \end{cases} \tag{12}$$

The ACs inform BC about the existence of anomaly by releasing $x_{AC}(t)$ molecules. The BC uses the following hypothesis test to detect anomaly

$$\begin{cases} \mathcal{W}_0: \ \sum_{m=1}^{M}\lambda_{BC,m} < k\bar{\lambda}_{BC} \\ \mathcal{W}_1: \ \sum_{m=1}^{M}\lambda_{BC,m} \ge k\bar{\lambda}_{BC} \end{cases} \tag{13}$$

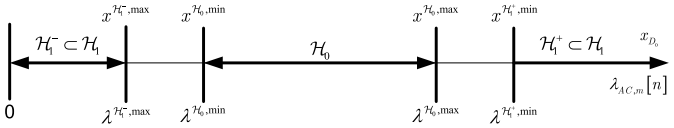

Fig. 2. Illustration of hypothesis test.

where $\mathcal{W}_0$ and $\mathcal{W}_1$ are events corresponding to $\mathcal{H}_0$ and $\mathcal{H}_1$ in the BC. k is the minimum numbers of ACs, which detect anomaly in the DC-ACs link. $\bar{\lambda}_{BC}$ is the average number of received molecules at the BC given $x_{AC,m}(t) = x_{AC_0}\exp(-\kappa' t^{b'})$ for $\forall m \in \{1,\ldots,M\}$, i.e.,

$$\bar{\lambda}_{BC} = \frac{1}{M}\sum_{m=1}^{M}\lambda_{BC,m}. \tag{14}$$

D. Problem Formulation

Given $\{y_{AC,m}[n]\}_{n=n_{ss}+1}^{n_{ss}+N}$, $\lambda_{AC,m}^{\mathcal{H}_0,\min}$, $\lambda_{AC,m}^{\mathcal{H}_0,\max}$, $\lambda_{AC,m}^{\mathcal{H}_1^+,\min}$, $\lambda_{AC,m}^{\mathcal{H}_1^-,\max}$ and an upper bound of probability of false alarm (P_F), β, find the probability of false alarm at m^{th} AC, i.e., $P_F^{AC,m}$, and decision threshold at BC, $y_{BC,m}^{\text{THR}}$, to maximize the probability of detection, P_D. The problem can be reformulated as following optimization problem

$$\begin{aligned} (\text{P1}) \quad & \max_{P_F^{AC,m}, y_{BC}^{\text{THR}}} \quad P_D\left(P_F^{AC,m}, y_{BC}^{\text{THR}}\right) \\ & s.t. \qquad P_F \le \beta \end{aligned} \tag{15}$$

where P_D and P_F are defined in two next sections and P1 denotes the problem 1 in this paper.

E. Assumptions

We now state precisely our modeling assumptions.

- AS1: Conditioned on hypothesis $\mathcal{H}_j$, $j \in \{0,1\}$, the observations at distinct ACs are independent.
- AS2: Conditioned on hypothesis $\mathcal{H}_j$, $j \in \{0,1\}$, the observations at each AC, $y_{AC,m}[n]$ for $n_{ss}+1 \le n \le n_{ss}+N$, are independent.
- AS3: AC measures the number of received molecules after time of t_{ss}.
- AS4: We assume $g_m(t;\tau)$s are equal and almost constant over time.
- AS5: We consider a symmetric topology for health monitoring network, hence $\bar{\eta}_m = \bar{\eta}$, probability of detection and false alarm in ACs are equal, i.e., $P_D^{AC,m} = P_D^{AC}$ and $P_F^{AC,m} = P_F^{AC}$.
- AS6: AC's are injected in the near location of cancer cells, and send their message to BC using the blood vessels medium.

III. ANOMALY DETECTION PERFORMANCE OF ACS

The NP framework needs to calculate the LR of hypothesis test. Calculating the LR test of hypothesis test in (12) needs the mean of $y_{AC,m}[n]$, i.e., $\lambda_{AC,m}[n]$, which is not known in our scenario. Hence to derive the decision rule of hypothesis

test the generalized likelihood ratio test (GLRT) is established and the decision rule is provided in the following proposition.

Proposition 1: The decision rule of the hypothesis test in (12) based on GLRT for the m^{th} AC with N independent Poisson observations is

$$\sum_{n=n_{ss}+1}^{n=n_{ss}+N} \hat{\lambda}_{AC,m}^{\mathcal{H}_0}[n] - \hat{\lambda}_{AC,m}^{\mathcal{H}_1}[n] + y_{AC,m}[n]\log\Big(\hat{\lambda}_{AC,m}^{\mathcal{H}_1}[n] + p_r\bar{\eta}\Big) - y_{AC,m}[n]\log\Big(\hat{\lambda}_{AC,m}^{\mathcal{H}_0}[n] + p_r\bar{\eta}\Big) \overset{\mathcal{H}_1}{>} \log\gamma \quad (16)$$

where γ can be derived by limiting the false alarm probability and $\hat{\lambda}_{AC,m}^{\mathcal{H}_0}[n]$ and $\hat{\lambda}_{AC,m}^{\mathcal{H}_1}[n]$ are derived as

$$\hat{\lambda}_{AC,m}^{\mathcal{H}_0}[n] = \begin{cases} \lambda_{AC,m}^{\mathcal{H}_0,\min} & y_{AC,m}[n] - p_r\bar{\eta} \le \lambda_{AC,m}^{\mathcal{H}_0,\min} \\ y_{AC,m}[n] - p_r\bar{\eta} & \lambda_{AC,m}^{\mathcal{H}_0,\min} \le y_{AC,m}[n] - p_r\bar{\eta} \le \lambda_{AC,m}^{\mathcal{H}_0,\max} \\ \lambda_{AC,m}^{\mathcal{H}_0,\max} & y_{AC,m}[n] - p_r\bar{\eta} \ge \lambda_{AC,m}^{\mathcal{H}_0,\max} \end{cases} \quad (17)$$

$$\hat{\lambda}_{AC,m}^{\mathcal{H}_1}[n] = \begin{cases} 0 & y_{AC,m}[n] - p_r\bar{\eta} < 0 \\ y_{AC,m}[n] - p_r\bar{\eta} & 0 \le y_{AC,m}[n] - p_r\bar{\eta} \le \lambda_{AC,m}^{\mathcal{H}_1^-,\max} \\ & \lambda_{AC,m}^{H_1^-,\max} \le y_{AC,m}[n] - p_r\bar{\eta} \\ \lambda_{AC,m}^{\mathcal{H}_1^-,\max} & < \dfrac{\lambda_{AC,m}^{\mathcal{H}_1^+,\min} - \lambda_{AC,m}^{\mathcal{H}_1^-,\max}}{\log\left(\dfrac{\lambda_{AC,m}^{\mathcal{H}_1^+,\min} + p_r\bar{\eta}}{\lambda_{AC,m}^{\mathcal{H}_1^-,\max} + p_r\bar{\eta}}\right)} \\ \lambda_{AC,m}^{\mathcal{H}_1^+,\min} & \dfrac{\lambda_{AC,m}^{\mathcal{H}_1^+,\min} - \lambda_{AC,m}^{\mathcal{H}_1^-,\max}}{\log\left(\dfrac{\lambda_{AC,m}^{\mathcal{H}_1^+,\min} + p_r\bar{\eta}}{\lambda_{AC,m}^{\mathcal{H}_1^-,\max} + p_r\bar{\eta}}\right)} \le y_{AC,m}[n] - p_r\bar{\eta} \\ & < \lambda_{AC,m}^{H_1^+,\min} \\ y_{AC,m}[n] - p_r\bar{\eta} & y_{AC,m}[n] - p_r\bar{\eta} \ge \lambda_{AC,m}^{\mathcal{H}_1^+,\min} \end{cases} \quad (18)$$

Proof: See Supplementary Materials, Appendix A. ∎

Calculating γ in Proposition 1, is not easy due to complexity to find the distribution of the test statistic in (16). Moreover, the test statistic is a nonlinear function of measurements, $y_{AC,m}[\cdot]$. Therefore, implementing (16) in an AC with limited complexity is challenging, hence, a simplified decision rule using bounding the likelihood ratio is proposed in the next theorem. We provide a lower bound on the probability of detection and an upper bound on the probability of false alarm. In the next theorem we need the ML estimate of $\lambda_{AC,m}[n]$, which is provided in the next lemma

Lemma 1: The ML estimator of $\lambda_{AC,m}[n]$ is given by

$$\hat{\lambda}_{AC,m}[n] = \max\big(y_{AC,m}[n] - p_r\bar{\eta}, 0\big). \quad (19)$$

Proof: See Supplementary Materials, Appendix B. ∎

The next theorem represents both the resulting simplified decision rule and a lower bound on the probability of detection for the hypothesis test (12).

Theorem 1: The simplified decision rule deceived from bounding likelihood ratio for the m^{th} AC with N independent Poisson observations and limited false alarm probability $P_F^{AC,m} < \xi_1$ is

$$\begin{cases} \mathcal{H}_0\text{:} & \max(\gamma_l, 0) \le \frac{1}{N}\sum_{n=n_{ss}+1}^{n_{ss}+N} y_{AC,m}[n] \le \gamma_u \\ \mathcal{H}_1\text{:} & \begin{cases} \frac{1}{N}\sum_{n=n_{ss}+1}^{n_{ss}+N} y_{AC,m}[n] > \gamma_u \\ \frac{1}{N}\sum_{n=n_{ss}+1}^{n_{ss}+N} y_{AC,m}[n] < \max(\gamma_l, 0) \end{cases} \text{or} \end{cases} \quad (20)$$

where

$$\gamma_l \coloneqq \lambda_{AC,m}^{\mathcal{H}_0,\min} + p_r\bar{\eta} - \gamma' \quad (21)$$

$$\gamma_u \coloneqq \lambda_{AC,m}^{\mathcal{H}_0,\max} + p_r\bar{\eta} + \gamma' \quad (22)$$

and γ' is the minimum value which satisfies the following inequalities

$$\frac{\Gamma\Big(\lfloor N\gamma_u + 1\rfloor, N\Big(\lambda_{AC,m}^{\mathcal{H}_0,\max} + p_r\bar{\eta}\Big)\Big)}{\lfloor N\gamma_u\rfloor!} - \frac{\Gamma\Big(\lceil\max(N\gamma_l - 1, 0) + 1\rceil, N\Big(\lambda_{AC,m}^{\mathcal{H}_0,\min} + p_r\bar{\eta}\Big)\Big)}{\lceil\max(N\gamma_l - 1, 0)\rceil!} \ge 1 - \xi_1, \quad (23)$$

where $\Gamma(c, s) \coloneqq \int_s^\infty z^{c-1}e^{-z}\mathrm{d}z$ is the incomplete Gamma function, $\lfloor\cdot\rfloor$ and $\lceil\cdot\rceil$ denote floor and ceiling functions respectively, and ! is the factorial operator.

The lower bound of the detection probability is obtained as

$$P_D^{AC,m} = \min\left(\frac{\Gamma\Big(\lceil\max(N\gamma_l - 1, 0) + 1\rceil, N\Big(\lambda_{AC,m}^{\mathcal{H}_1^-,\max} + p_r\bar{\eta}\Big)\Big)}{\lceil\max\{N\gamma_l - 1, 0\}\rceil!}, 1 - \frac{\Gamma\Big(\lfloor N\gamma_u + 1\rfloor, N\Big(\lambda_{AC,m}^{\mathcal{H}_1^+,\min} + p_r\bar{\eta}\Big)\Big)}{\lfloor N\gamma_u\rfloor!}\right) \quad (24)$$

where the $\min(\cdot,\cdot)$ is minimum function.

Proof: See Supplementary Materials, Appendix C. ∎

IV. Anomaly Detection Performance at the BC

In this section a lower bound for total probability of detection and an upper bound for total probability of false alarm of the health monitoring network is derived. If the ACs-BC link is perfect the presence of anomaly is alarmed when at least k numbers of ACs alarm the hypothesis $\mathcal{H}_1$ by transmitting $x_{AC,m}(t)$ molecules.

By assuming independent observations for the ACs and a symmetric topology for the network, the probabilities of detection and false alarm at the ACs would be equal, i.e., $P_D^{AC,m} = P_D^{AC}$, $P_F^{AC,m} = P_F^{AC}$. The next theorem represents the decision rule at the BC and the total probabilities of detection and false alarm for the health monitoring network considering a symmetric topology.

Theorem 2: The decision rule for the BC with Poisson observation is

$$\begin{cases} \mathcal{H}_0 : \ y_{BC} < y_{BC}^{\text{THR}} \\ \mathcal{H}_1 : \ y_{BC} \ge y_{BC}^{\text{THR}} \end{cases} \quad (25)$$

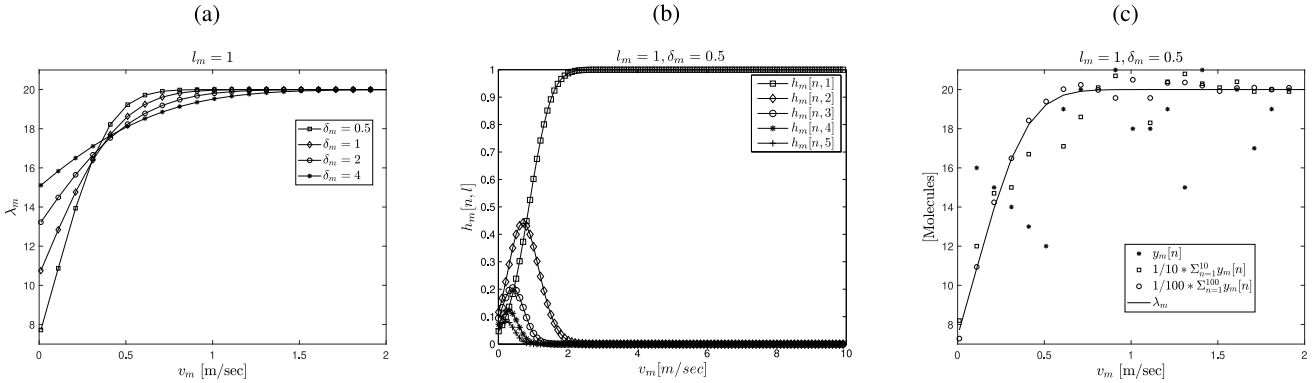

Fig. 3. Average number of received molecules in the receiver (λ_m) in terms of drift velocity (v_m) for different values of coefficient of diffusion (δ_m) (b) The channel coefficient, $h_m(n,l)$, $l \in \{1,\ldots,5\}$ in terms of drift velocity (v_m) (c) comparison of sample mean of number of received molecules for different length of averaging with average number of received molecules in the receiver (λ_m) all with $l_m = 1$, $\delta_m = 0.5$ and sending 20 molecules at the transmitter.

The derived lower bound of probability detection and upper bound for probability of false alarm at the BC are

$$P_D = \sum_{m=0}^{M} p'_m \left(1 - \frac{\Gamma\left(\lceil y_{BC}^{\mathrm{THR}} \rceil, m\bar{\lambda}_{BC} + q_r\bar{\varepsilon}\right)}{\lceil y_{BC}^{\mathrm{THR}} - 1 \rceil !}\right) \quad (26)$$

$$P_F = \sum_{m=1}^{M} p''_m \left(1 - \frac{\Gamma\left(\lceil y_{BC}^{\mathrm{THR}} \rceil, m\bar{\lambda}_{BC} + q_r\bar{\varepsilon}\right)}{\lceil y_{BC}^{\mathrm{THR}} - 1 \rceil !}\right) \quad (27)$$

where y_{BC}^{THR} is the decision threshold at the BC. In addition, p'_m and p''_m denote the probability of detecting anomaly at m ACs, under $\mathcal{H}_1$ and $\mathcal{H}_0$, respectively, which are given by

$$p'_m = \binom{M}{m}\left(1 - P_D^{AC}\right)^{M-m}\left(P_D^{AC}\right)^{m} \quad (28)$$

$$p''_m = \binom{M}{m}\left(1 - P_F^{AC}\right)^{M-m}\left(P_F^{AC}\right)^{m} \quad (29)$$

Proof: The proof is provided in Supplementary Materials, Appendix D. ∎

Our initial goal was solving P1. Due to there is no computational efficient closed form for P_D in (15); we derived a lower bound of probability of detection in (26) and an upper bound for probability of false alarm in (27), based on which we solve P1. Due to the non-linear complex nature of these functions, we will solve the P1 numerically in the next section.

By the following lemma it is easy to show that the optimization problem (15) can be reduced to an equality constraint optimization problem.

Lemma 2: The optimal value of P_D is attained for $P_F = \beta$.

Proof: Assuming P_F^{AC} to be a constant, P_D is monotonically decreasing function of y_{BC}^{THR}. Therefore the optimal P_D is attained for the lowest y_{BC}^{THR} in the feasible set of (P1). Furthermore, P_F is monotonically decreasing function of y_{BC}^{THR}, therefore, the lowest y_{BC}^{THR} in the feasible set of (P1) is attained for $P_F = \beta$.

Now assume that $\exists(y_{BC}^{\mathrm{THR}^*}, P_F^{AC^*})$ such that $P_F^* < \beta$ and P_D^* is optimal solution of (P1). According to above statement, there is a $y_{BC}^{\mathrm{THR}^{**}} < y_{BC}^{\mathrm{THR}^*}$ for which $P_F^{**} = \beta$ and $P_D^{**} > P_D^*$ which is contradiction. Hence the optimal P_D is attained for $P_F = \beta$. ∎

TABLE II
PARAMETERS OF NUMERICAL TEST

Symbol	Description	value
M	No. of ACs	30
N	No. of observations at ACs	[5 10 20 40 80 160]
$\bar{\epsilon}_{\mathrm{r}}$	Noise mean at BC	100
$\bar{\eta}$	Noise mean at ACs	20
p_r	Reception probability at ACs	0.05
q_r	Reception probability at BC	0.05
$y_{\mathrm{BC}}^{\mathrm{THR}}$	Decision threshold at BC	varies with unit of x_{AC_0} molecules
Δ_λ	$\min\left(\left\lvert\lambda_{AC,m}^{\mathcal{H}_1^-,\max} - \lambda_{AC,m}^{\mathcal{H}_0,\min}\right\rvert, \left\lvert\lambda_{AC,m}^{\mathcal{H}_1^+,\min} - \lambda_{AC,m}^{\mathcal{H}_0,\max}\right\rvert\right)$	[0.5 1 1.5 2]
$\lambda_{AC,m}^{\mathcal{H}_0,\min}$	Lower bound of $\lambda_{AC,m}[n]$ under $\mathcal{H}_0$	10
$\lambda_{AC,m}^{\mathcal{H}_0,\max}$	Upper bound of $\lambda_{AC,m}[n]$ under $\mathcal{H}_0$	20
$P_F^{AC,m}$	False alarm probability at m^{th} AC	$[10^{-4} - 10^{-1}]$

V. NUMERICAL TESTS

This section provides the numerical tests to assess the performance of the proposed health monitoring network. The effect of different parameters including, the number of observations at each AC, N, the decision thresholds at the BC, y_{BC}^{THR}, probability of false alarm at ACs, $P_F^{AC,m}$, and noise level at the BC, $\bar{\epsilon}_r$, on the performance are investigated. We used results of (23) and (24) in Theorem 1 and (26)-(29) in Theorem 2 to plot figures in this section. Table II represents the parameters of the numerical tests and associated values of parameters.

To assess the effects of channel parameters like drift velocity (v_m), coefficient of diffusion (δ_m), on the average number of received molecules (λ_m) we performed a computer simulation. Fig. 3(a) shows the λ_m in terms of v_m for different values of δ_m with $l_m = 1$ and the number of transmitted molecules is equal to 20. It can be observed that by increasing the v_m, λ_m is increased and finally converges to 20 molecules. Moreover, we can see that λ_m is increasing function in terms of δ_m for $v_m < 0.3$, and a decreasing function in terms of δ_m for $v_m > 0.3$. Fig. 3(b) shows the channel coefficient, $h_m[n,l]$, $l \in \{1,\ldots,5\}$ in terms of v_m with $l_m = 1$, $\delta_m = 0.5$. The

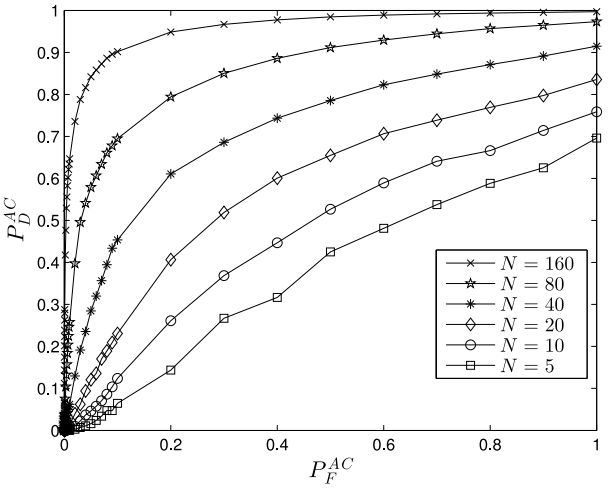

Fig. 4. P_D^{AC} in terms of P_F^{AC} for different values of N, $\Delta_\lambda = 1$.

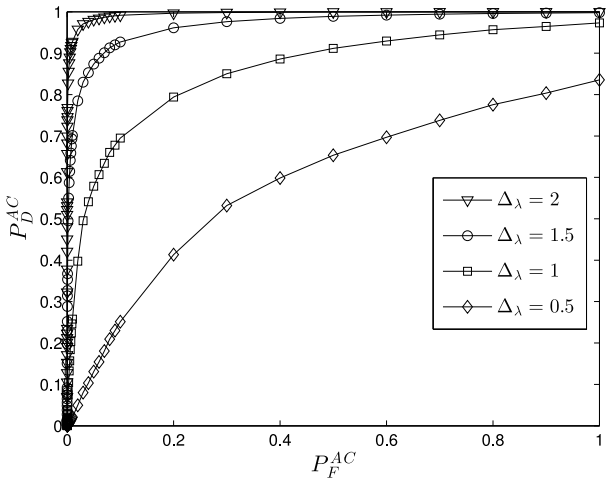

Fig. 5. P_D^{AC} in terms of P_F^{AC} for different values of Δ_λ, and $N = 80$.

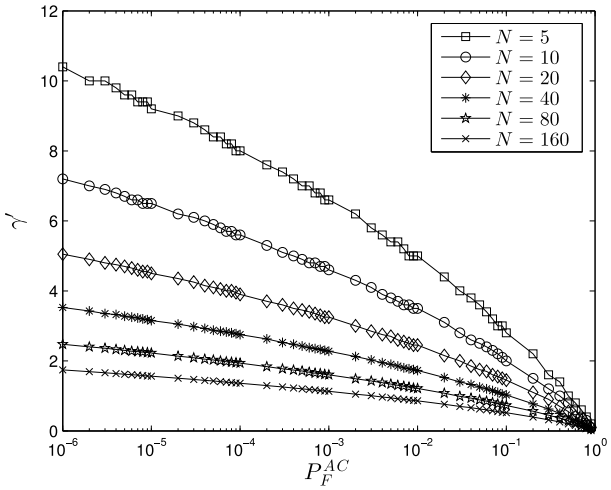

Fig. 6. γ' in terms of P_F^{AC} for different values of N and $\Delta_\lambda = 1$.

probability of receiving molecules in same time slot converges to 1 for $v_m > 2.5$. Fig. 3(c) compare the sample mean of number of received molecules for different length of averaging derived from computer simulations with λ_m. In computer

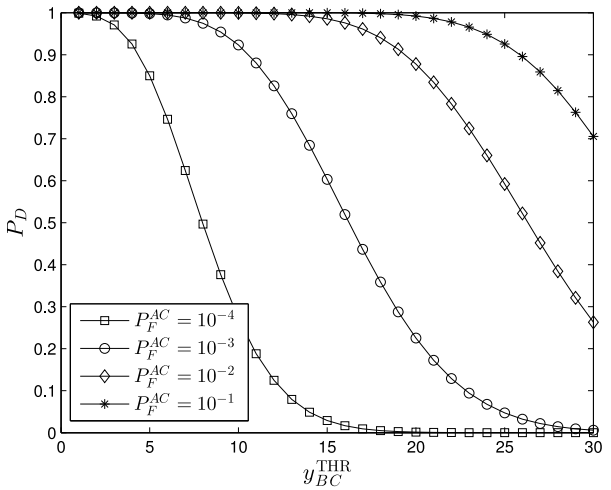

Fig. 7. P_D in terms of y_{BC}^{THR} for different values of P_F^{AC}, $\Delta_\lambda = 1$ and $\bar{\varepsilon} = 100$.

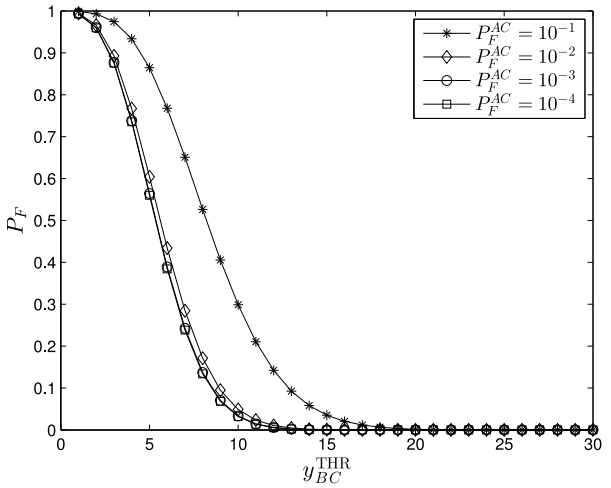

Fig. 8. P_F in terms of y_{BC}^{THR} for different values of P_F^{AC}, $\Delta_\lambda = 1$ and $\bar{\varepsilon} = 100$.

simulations, $l_m = 1$, $\delta_m = 0.5$, and the number of transmitted molecules is 20. It can be seen the sample mean of number of received molecules converges to λ_m by increasing the time of performing sample mean from the number of received molecules. For specific value of $l_{m,\min} \leq l_m \leq l_{m,\max}$, $v_{m,\min} \leq v_m(t) \leq v_{m,\max}$ and $\sigma^2_{m,min} \leq \sigma^2_m(t) \leq \sigma^2_{m,\max}$, $\lambda_{AC,m}[n]$ are derived. The $\lambda_{AC,m}^{\mathcal{H}_{0,\max}}$ and $\lambda_{AC,m}^{\mathcal{H}_{0,min}}$ are

$$\lambda_{AC,m}^{\mathcal{H}_{0,\max}} = \max \Big(\lambda_{AC,m}^{\mathcal{H}_0}\Big(l_{m,\min}, v_{m,\max}, \sigma^2_{m,\min}\Big), \lambda_{AC,m}^{\mathcal{H}_0}\Big(l_{m,\min}, v_{m,\max}, \sigma^2_{m,max}\Big)\Big) \quad (30)$$

$$\lambda_{AC,m}^{\mathcal{H}_{0,\min}} = \min \Big(\lambda_{AC,m}^{\mathcal{H}_0}\Big(l_{m,\max}, v_{m,\min}, \sigma^2_{m,\min}\Big), \lambda_{AC,m}^{\mathcal{H}_0}\Big(l_{m,\max}, v_{m,\min}, \sigma^2_{m,max}\Big)\Big) \quad (31)$$

In a similar way, $\lambda_{AC,m}^{\mathcal{H}_{1,\max}^+}$, $\lambda_{AC,m}^{\mathcal{H}_{1,\max}^-}$ are derived.

In Fig. 4 the proposed lower bound for probability of detection of the AC, P_D^{AC} in (24), versus the upper bound of

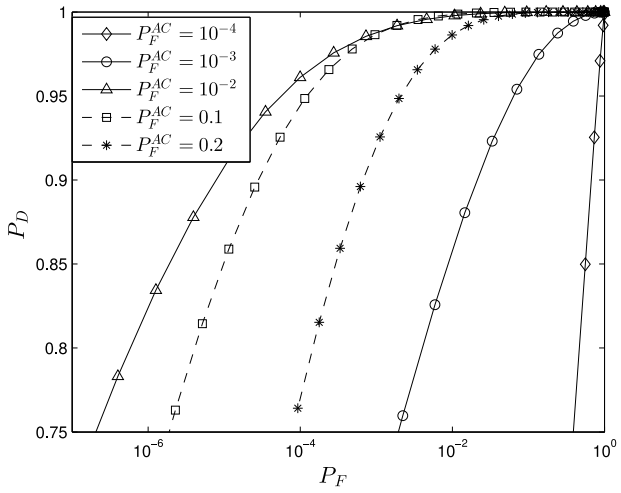

Fig. 9. P_D in terms of P_F for different values of P_F^{AC}, $\Delta_\lambda = 1$ and $\bar{\varepsilon} = 100$.

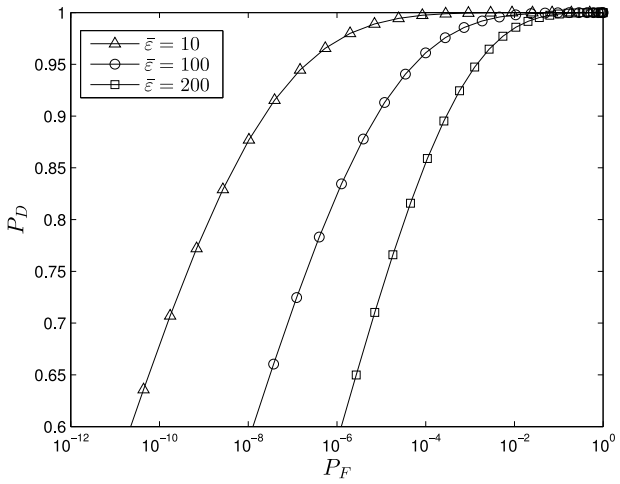

Fig. 11. P_D in terms of P_F for different values of $\bar{\varepsilon}$, $\Delta_\lambda = 1$ and $P_F^{AC} = 10^{-2}$.

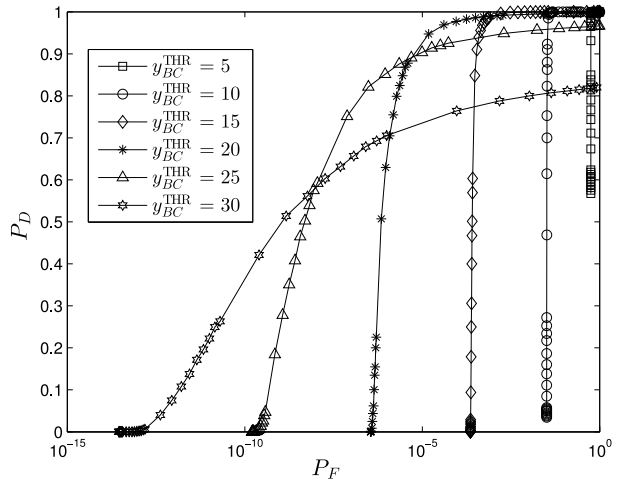

Fig. 10. P_D in terms of P_F for different values of y_{BC}^{THR}, $N = 80$, $\Delta_\lambda = 1$ and $P_F^{AC} = 10^{-1}$.

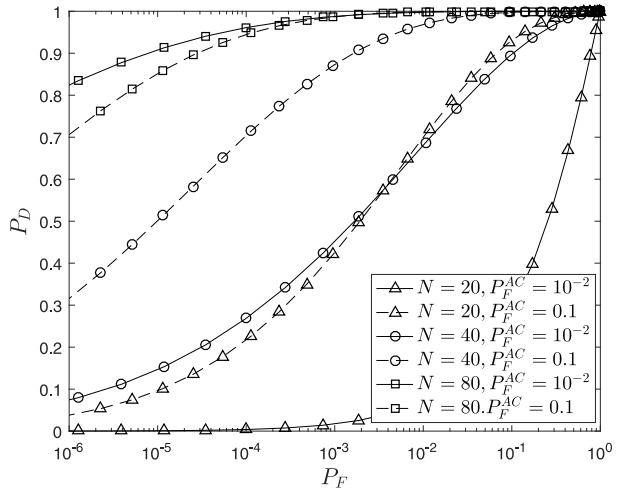

Fig. 12. P_D in terms of P_F for different values of N and $P_F^{AC} = 10^{-2}$ and $\Delta_\lambda = 1$.

probability of false alarm of the AC, P_F^{AC}, for different number of observations at the AC, N, is depicted. As it is evident P_D^{AC} is an increasing function of N and P_F^{AC}.

Similarly, in Fig. 5 the P_D^{AC}, versus P_F^{AC} for different values of Δ_λ is depicted, Δ_λ quantifies the level of deviation of $\lambda_{AC,m}[n]$ in non healthy setting with that in the healthy setting. Δ_λ is defined as follows

$$\Delta_\lambda \coloneqq \min\left(\left|\lambda_{AC,m}^{\mathcal{H}_1^-,\max} - \lambda_{AC,m}^{\mathcal{H}_0,\min}\right|, \left|\lambda_{AC,m}^{\mathcal{H}_1^+,\min} - \lambda_{AC,m}^{\mathcal{H}_0,\max}\right|\right) \tag{32}$$

Clearly, as it is expected that P_D^{AC} is an increasing function of Δ_λ and $P_F^{AC,m}$ is a decreasing function of Δ_λ.

Fig. 6 depicts thresholds of AC; γ' in terms of P_F^{AC} for different values of N. It can be observed that by increasing N, variation of γ' in terms of P_F^{AC} is reduced. Using this figure by knowing P_F^{AC}, the value of threshold at AC is obtained.

In Fig. 7 the lower bound of total probability of detection, P_D, is depicted versus y_{BC}^{THR} for different values of P_F^{AC}. As it is evident, P_D is a decreasing function of y_{BC}^{THR} while it is an increasing function of P_F^{AC}.

Similarly, in Fig. 8 the upper bound for total probability of false alarm, P_F, is depicted versus y_{BC}^{THR} for different values of P_F^{AC}. Clearly, P_F is a decreasing function of y_{BC}^{THR} and an increasing function of P_F^{AC}. For smaller values of P_F^{AC} (likely < 10^{-2}) the DC-AC channel is error free when hypothesis of $\mathcal{H}_0$ is occurred, and the AC-BC channel has dominant effect on P_F, but for larger values of P_F^{AC} the effect of performance of DC-AC channel on P_F is more dominant. It is the reason when we change the P_F^{AC} from 10^{-2} to 10^{-1} we observe a shift on the P_F to right side.

Fig. 7 and 8, can lead to find the optimal value of y_{BC}^{THR} which maximizes P_D and limit P_F for a given P_F^{AC}.

It is noteworthy that to plot the subsequent figures, P_F^{AC} is changed when y_{BC}^{THR} is fixed and vise versa.

Fig. 9 depicts the receiver operating characteristic of the BC, for different P_F^{AC}. As it can be seen, for $P_F^{AC} < 0.01$, the higher values of P_F^{AC} provides the better the performance of the health monitoring network, while for $P_F^{AC} > 0.01$ by

increasing P_F^{AC}, the performance is degraded. Hence, for the selected parameters, the approximated optimal value for P_F^{AC} is $P_F^{AC} = 0.01$.

Fig. 10 depicts the receiver operating characteristic of the BC, for different values of y_{BC}^{THR}. It has been plotted by varying P_F^{AC} in each curve. As it can be seen, by increasing y_{BC}^{THR}, P_D is improved for $y_{BC}^{\mathrm{THR}} < 15$ and $P_F > 10^{-6}$, also P_D is degraded for $y_{BC}^{\mathrm{THR}} > 15$ and $P_F > 10^{-6}$.

Fig. 11 investigates the effect of noise intensity at the BC, $\bar{\varepsilon}$, on the detection performance. It can be inferred that for a given value of P_F, decreasing the level of noise increases the lower bound of detection probability, P_D.

Fig. 12 depicts the receiver operation characteristic of the BC, for different values of N and P_F^{AC}, it can be observed that, performance of detection is improved by increasing the N. It can be observed, by increasing P_F^{AC} from 10^{-2} to 10^{-1}, P_D is improved with $N = 20$ and $N = 40$, while by increasing P_F^{AC} from 10^{-2} to 10^{-1}, P_D is degraded for $N = 80$.

VI. Conclusion

In this paper an anomaly detection scheme in a two-tier bio-molecular network was proposed. Released biomarkers by DCs serve as a detection feature for the ACs to detect any anomalies. The ACs, at the first tier, act as receivers over an MC channel. Then the ACs communicate with a BC over a second MC channel. Based on bounding likelihood ratio a lower bound for probability of detection and an upper bound for false alarm of each AC was derived. Next, the total detection performance, at the BC, was quantified using lower bound of detection probability and upper bound of false alarm at ACs. Finally, a design problem was set up which quantifies the decision thresholds of the ACs and BC to maximize a lower bound of total probability of detection. The results indicate how effective fusion of noisy observations collected from a number of ACs with limited capabilities could provide an acceptable detection performance.

Acknowledgment

The author would like to thank Alireza Sadeghi for his valuable comments and fruitful discussions.

References

[1] I. F. Akyildiz, M. Pierobon, S. Balasubramaniam, and Y. Koucheryavy, "The Internet of Bio-Nano Things," *IEEE Comm. Mag.*, vol. 53, no. 3, pp. 32–40, Mar. 2015.

[2] S. Ghavami, F. Lahouti, and A. Masoudi-Nejad, "Modeling and analysis of abnormality detection in biomolecular nano-networks," *Nano Commun. Netw.*, vol. 3, no. 4, pp. 229–241, Dec. 2012.

[3] G. E. Santagati, T. Melodia, L. Galluccio, and S. Palazzo, "Ultrasonic networking for E-health applications," *IEEE Wireless Commun.*, vol. 20, no. 4, pp. 74–81, Aug. 2013.

[4] X. Fu *et al.*, "A wireless implantable sensor network system for in vivo monitoring of physiological signals," *IEEE Trans. Inf. Technol. Biomed.*, vol. 15, no. 4, pp. 577–584, Jul. 2011.

[5] X. Wu *et al.*, "Immunofluorescent labeling of cancer marker Her2 and other cellular targets with semiconductor quantum dots," *Nat. Biotechnol.*, vol. 21, no. 1, pp. 41–46, 2003.

[6] J. K. Jaiswal, H. Mattoussi, J. M. Mauro, and S. M. Simon, "Long-term multiple color imaging of live cells using quantum dot bioconjugates," *Nat. Biotechnol.*, vol. 21, no. 1, pp. 47–51, 2003.

[7] X. Huang *et al.*, "A reexamination of active and passive tumor targeting by using rod-shaped gold nanocrystals and covalently conjugated peptide ligands," *ACS Nano*, vol. 4, no. 10, pp. 5887–5896, 2010.

[8] R. Levy, U. Shaheen, Y. Cesbron, and V. See, "Gold nanoparticles delivery in mammalian live cells: A critical review," *Nano Rev.*, vol. 1, p. 4889, Feb. 2010.

[9] S. Ghavami and F. Lahouti, "Abnormality detection in correlated Gaussian molecular nano-networks: Design and analysis," *IEEE Trans. NanoBiosci.*, vol. 16, no. 3, pp. 189–202, Apr. 2017.

[10] R. Mosayebi, A. Ahmadzadeh, W. Wicke, V. Jamali, R. Schober, and M. Nasiri-Kenari, "Early cancer detection in blood vessels using mobile nanosensors," *IEEE Trans. NanoBiosci.*, vol. 18, no. 2, pp. 103–116, Apr. 2019.

[11] N. Varshney, A. Patel, Y. Deng, W. Haselmayr, P. K. Varshney, and A. Nallanathan, "Abnormality detection inside blood vessels with mobile nanomachines," *IEEE Trans. Mol. Biol. Multi-Scale Commun.*, vol. 4, no. 3, pp. 189–194, Sep. 2018.

[12] R. Mosayebi, W. Wicke, V. Jamali, A. Ahmadzadeh, R. Schober, and M. Nasiri-Kenari, "Advanced target detection via molecular communication," in *Proc. IEEE Global Commun. Conf. (GLOBECOM)*, Abu Dhabi, UAE, Dec. 2018, pp. 1–7.

[13] Y. Fang, A. Noel, N. Yang, A. W. Eckford, and R. A. Kennedy, "Distributed cooperative detection for multi-receiver molecular communication," in *Proc. IEEE Global Telecomm. Conf.*, Washington, DC, USA, Dec. 2016, pp. 1–7.

[14] R. Mosayebi, V. Jamali, N. Ghoroghchian, R. Schober, M. Nasiri-Kenari, and M. Mehrabi, "Cooperative abnormality detection via diffusive molecular communications," *IEEE Trans. NanoBiosci.*, vol. 16, no. 8, pp. 828–842, Dec. 2017.

[15] Y. Fang, A. Noel, N. Yang, A. W. Eckford, and R. A. Kennedy, "Symbol-by-symbol maximum likelihood detection for cooperative molecular communication," *IEEE Trans. Commun.*, vol. 67, no. 7, pp. 4885–4899, Jul. 2019.

[16] N. Ghoroghchian, M. Mirmohseni, and M. Nasiri-Kenari, "Abnormality detection and monitoring in multi-sensor molecular communication," *IEEE Trans. Mol. Biol. Multi-Scale Commun.*, vol. 5, no. 2, pp. 68–83, Nov. 2019.

[17] T. C. Mai, M. Egan, T. Q. Duong, and M. Di Renzo, "Event detection in molecular communication networks with anomalous diffusion," *IEEE Commun. Lett.*, vol. 21, no. 6, pp. 1249–1252, Jun. 2017.

[18] S. Galmés, "Cardiovascular system monitoring via wireless nanosensor networks," in *Cooperative Design, Visualization, and Engineering*, Y. Luo, Ed. Cham, Switzerland: Springer, 2019, pp. 39–44.

[19] O. D. Kose, M. C. Gursoy, M. Saraclar, A. E. Pusane, and T. Tugcu, "Machine learning-based silent entity localization using molecular diffusion," *IEEE Commun. Lett.*, vol. 24, no. 4, pp. 807–810, Apr. 2020.

[20] C. D. Pahlajani, I. Poulakakis, and H. G. Tanner, "Networked decision making for Poisson processes with applications to nuclear detection," *IEEE Trans. Autom. Control*, vol. 59, no. 1, pp. 193–198, Jan. 2014.

[21] R. J. Nemzek, J. S. Dreicer, D. C. Torney, and T. T. Warnock, "Distributed sensor networks for detection of mobile radioactive sources," *IEEE Trans. Nucl. Sci.*, vol. 51, no. 4, pp. 1693–1700, Aug. 2004.

[22] C. D. Pahlajani, J. Sun, I. Poulakakis, and H. G. Tanner, "Error probability bounds for nuclear detection: Improving accuracy through controlled mobility," *Automatica*, vol. 50, no. 10, pp. 2470–2481, 2014.

[23] C. D. Pahlajani, J. Sun, I. Poulakakis, and H. G. Tanner, "Performance bounds for mismatched decision schemes with Poisson process observations," *Syst. Control Lett.*, vol. 75, pp. 69–76, Jan. 2015.

[24] C. D. Pahlajani, J. Sun, I. Poulakakis, and H. G. Tanner, "Error probabilities and threshold selection in networked nuclear detection," in *Proc. 52nd IEEE Conf. Decis. Control*, Florence, Italy, Dec. 2013, pp. 5450–5455.

[25] J. Sun, H. G. Tanner, and I. Poulakakis, "Active sensor networks for nuclear detection," in *Proc. IEEE Int. Conf. Robot. Autom.*, Seattle, WA, USA, May 2015, pp. 3549–3554.

[26] C. D. Pahlajani, I. Poulakakis, and H. G. Tanner, "Decision-making accuracy for networks of sensors observing time-inhomogenous Poisson processes," in *Proc. IEEE Int. Conf. Robot. Autom.*, 2016, pp. 177–190.

[27] I. F. Akyildiz, F. Brunetti, and C. Blázquez, "Nanonetworks: A new communication paradigm," *Comput. Netw.*, vol. 52, no. 12, pp. 2260–2279, 2008.

[28] G. E. Santagati, T. Melodia, L. Galluccio, and S. Palazzo, "Medium access control and rate adaptation for ultrasonic intrabody sensor networks," *IEEE/ACM Trans. Netw.*, vol. 23, no. 4, pp. 1121–1134, Aug. 2015.

[29] H. Guo, P. Johari, J. M. Jornet, and Z. Sun, "Intra-body optical channel modeling for in vivo wireless nanosensor networks," *IEEE Trans. NanoBiosci.*, vol. 15, no. 1, pp. 41–52, Jan. 2016.
[30] L. Felicetti, M. Femminella, G. Reali, and P. Liò, "A molecular communication system in blood vessels for tumor detection," in *Proc. ACM 1st Annu. Int. Conf. Nanoscale Comput. Commun.*, Atlanta, GA, USA, 2014, pp. 1–9.
[31] S. Damani *et al.*, "Characterization of circulating endothelial cells in acute myocardial infarction," *Sci. Transl. Med.*, vol. 4, no. 126, pp. 126–133, 2012.
[32] V. Papadopoulou, K. Kosmidis, M. Vlachou, and P. Macheras, "On the use of the weibull function for the discernment of drug release mechanisms," *Int. J. Pharmaceutics*, vol. 309, nos. 1–2, pp. 44–50, 2006.
[33] Y. Chahibi and I. F. Akyildiz, "Molecular communication noise and capacity analysis for particulate drug delivery systems," *IEEE Trans. Commun.*, vol. 62, no. 11, pp. 3891–3903, Nov. 2014.
[34] K. V. Srinivas, A. W. Eckford, and R. S. Adve, "Molecular communication in fluid media: The additive inverse gaussian noise channel," *IEEE Trans. Inf. Theory*, vol. 58, no. 7, pp. 4678–4692, Jul. 2012.
[35] S. Ghavami, R. S. Adve, and F. Lahouti, "Information rates of ASK-based molecular communication in fluid media," *IEEE Trans. Mol. Biol. Multi-Scale Commun.*, vol. 1, no. 3, pp. 277–291, Sep. 2015.

Siavash Ghavami (Member, IEEE) received the B.S. and M.S. degrees (with Hons.) in electrical engineering from the Iran University of Science and Technology, Tehran, Iran, in 2006 and 2009, respectively, and the Ph.D. degree in electrical engineering from the University of Tehran, in 2014. Between 2012 and 2014, he worked first as a Research Scholar with the Laboratory of Adaptive and Regenerative Software Systems, and the Department of System Biology and Bioinformatics, both in Faculty of Computer Science and Electrical Engineering, University of Rostock, Rostock, Germany, and subsequently a Research Scholar with the School of Electrical and Computer Engineering (ECE), University of Toronto, Toronto, ON, Canada. Between 2015 and 2019, he served as a Postdoctoral Associate with the School of ECE, University of Minnesota, Minneapolis, MN, USA, and as a Research Fellow with the Department of Radiology, College of Science and Medicine, Mayo Clinic, Rochester, MN, USA. His research interests include statistical signal processing, wireless communications, coding and information theory, machine learning, molecular and neuronal communications, and mathematical modeling in biomedical engineering.